

Phase behavior and dynamic heterogeneities in lipids: A coarse-grained simulation study of DPPC–DPPE mixtures

Brian Y. Wong, Roland Faller *

Department of Chemical Engineering and Materials Science, UC Davis, Davis, CA 95616, USA

Received 12 August 2006; received in revised form 29 November 2006; accepted 6 December 2006

Available online 20 December 2006

Abstract

The coarse-grained Marrink-model for biomembrane simulation is used to study mixtures of dipalmitoylphosphatidylcholine (DPPC) and dipalmitoylphosphatidylethanolamine (DPPE) at various concentrations and temperatures. At high temperatures close to ideal mixing is observed. In the low temperature ordered phase dynamic heterogeneities are identified under some conditions. These are correlated with heterogeneities in the local order and define local neighborhoods.

© 2006 Elsevier B.V. All rights reserved.

Keywords: DPPC; DPPE; Lipid mixtures; Molecular simulation

1. Introduction

Computer simulations of biomembranes have become commonplace over the last decade [1–6]. Most simulations are using highly detailed atomistic simulations to elucidate the local structure of the membrane. However, in order to describe phase and mixing behaviors of different phospholipids we need coarse-grained descriptions to reach into the relevant time and length scales. One particularly successful mesoscale model has been proposed by Marrink et al. [7]. It has been shown e.g. that this model is capable of describing the phase coexistence of phospholipids [8]. It is designed to semiquantitatively compare to experimental data like area per molecule or membrane thickness while being computationally cheap enough to reach the microsecond timescale.

Cell membranes and correspondingly a number of model bilayers contain more than one type of phospholipid. In lipid mixtures, generally bilayer phases of various degrees of order coexist and form patterns [9]. Careful experimental studies in model mixtures have been performed [10–15] and patterns of various shapes have been found; among these stripes, circular

domains and long range hexagonal ordering [16–20]. Recently, simulations of phospholipid mixtures have come into focus [5,8,21–25] and have been successful in modeling phase coexistence in mixed bilayers [5,8,23,24] mostly based on simplified models of amphiphilic molecules [7,26–32]. Domain formation and qualitatively accurate domain sizes have been predicted using simple lattice models [33–35] where the coexistence of domains of different sizes has been shown [34]. Dynamical heterogeneities in bilayers, e.g. obstructed diffusion in heterogeneous phase separated systems where the more ordered phase acts as obstacles to the motion of the mobile lipids, have been established [12,15]. Very recently a Monte Carlo study has confirmed this scenario in a lattice model [36]. A wide variety of experiments has focused on model membrane systems to simplify the understanding of the structure of real cell membranes. Studies on giant unilamellar vesicles (GUVs) [37] and supported bilayers [12,14,38,39] are able to describe phase coexistence.

The biological most important patterns are so-called lipid rafts [9,40–46]. A raft is a specialized membrane domain composed mainly of cholesterol and sphingolipids. Rafts are tightly packed patches of lipids and cholesterol and can be viewed as floating cohesive units within loosely packed membrane components [45–47]. The general belief is that such rafts are on the order of 50 nm in diameter and therefore extremely difficult to directly observe experimentally [44].

* Corresponding author.

E-mail address: rfaller@ucdavis.edu (R. Faller).

Table 1
Overview of simulated systems

DPPC mol	DPPE mol	T [K]
128	0	310
96	32	285, 310
64	64	285, 310, 320, 330, 400
32	96	285, 310
0	128	285, 310

Rafts are believed to play an important role in cell signaling [48]. The general understanding of mixed bilayers and their domain structure is clearly a prerequisite to understanding the formation, stability, and biological function of rafts. Experimentally, rafts or lipid domains of varying degree of order have been characterized by a range of techniques. Confocal microscopy could visualize domains in mixtures of lipids of different lengths [49]. With fluorescence recovery after photobleaching (FRAP) mobility inhomogeneities in sperm cells [50] and in model systems [12] could be determined. Sizes of domains in model systems could be characterized by atomic force microscopy [12,38].

Two of the most abundant families of lipids are phosphatidylcholines and phosphatidylethanolamines, making mixtures of these a worthwhile topic of investigation. In this contribution we study a mixture of DPPE (dipalmitoylphosphatidylethanolamine) and DPPC (dipalmitoylphosphatidylcholine), both of which have the same chain length and are fully saturated. We first describe the overall characteristics of the bilayer and establish the mixing behavior depending on temperature before we study the correlation of local static and dynamic heterogeneities. Experimentally the phase diagram has been determined and it has been shown that with increasing DPPE content the phase transition temperature rises and the average lipid order increases [37,51,52]. Recently this system has been studied in atomistic detail [53] but that study did not focus on the phase behavior. The experimental phase transition temperatures of the pure systems are 337 K for DPPE and 314 K for DPPC respectively [52]. However, our simulation temperatures are lower as the model we are using is known to underestimate transition temperatures [8].

2. Materials and methods

Computer simulations have been performed with the Gromacs (V3.2) simulation suite [54]. The simulations contain 128 lipids with molar concentrations ranging from 0:100, 25:75, 50:50, 75:25, and 100:0 between DPPC and DPPE. We use the coarse-grained Marrink model [7]. Simulations are performed for 1 μ s with a time-step of 0.04 ps at 285 K, 310 K, 320 K, 330 K, and 400 K where temperature and pressure are controlled using Berendsen's weak coupling method [55] with time constants of 1.0 ps (non-rescaled times, see below). We use anisotropic coupling for the pressure control. We write conformations out every 1,000 simulation time-steps for subsequent analysis. A summary of all simulations is shown in Table 1. For most of the simulations the lipids were assigned randomly to the different leaflets leading to slightly imbalanced transbilayer distributions, e.g. 29:35 instead of 32:32 lipids in the equimolar mixture. We, additionally, performed a set of simulations for the equimolar concentrations with exactly balanced concentrations in both leaflets. The results as will be shown below do not show significant differences.

The model has been discussed in detail in a number of publications [7,8,56,57] so we only summarize its main features and focus on the difference between the lipids. In this model typically 4 heavy atoms and the corresponding hydrogens are subsumed into one interaction site. The lipids consist of apolar tails for the hydrocarbons, non-polar sites for the glycosidic backbone and polar sites for the headgroups. The difference between the PC and the PE lipids is exclusively the interaction site representing the choline or amine group respectively. The amine group has hydrogen bonding capabilities (both as a donor and an acceptor) whereas the choline group lacks these. This leads to a stronger mutual attraction of DPPE headgroups with respect to DPPC headgroups. Thus, we expect a tighter packing and higher order for the ethanolamines. All dynamics below is discussed in rescaled time where the time scale is fixed with the water diffusion constant. The corresponding scaling factor is 4.

3. Results

3.1. Statics

We measure the area per molecule of the system (cf. Fig. 1) and find that at 310 K the area rises linearly with increasing DPPC concentration indicating a close to ideal mixing between the lipids. However, at the lower temperature of 285 K we see that there is a slight minimum in area per lipid for close to the equimolar concentration and in general a much weaker dependence of the area on concentration indicating a transition to non-ideal mixing. Additionally, the clearly lower area per molecule at 285 K together with the relatively linear dependence of area per molecule versus temperature at higher

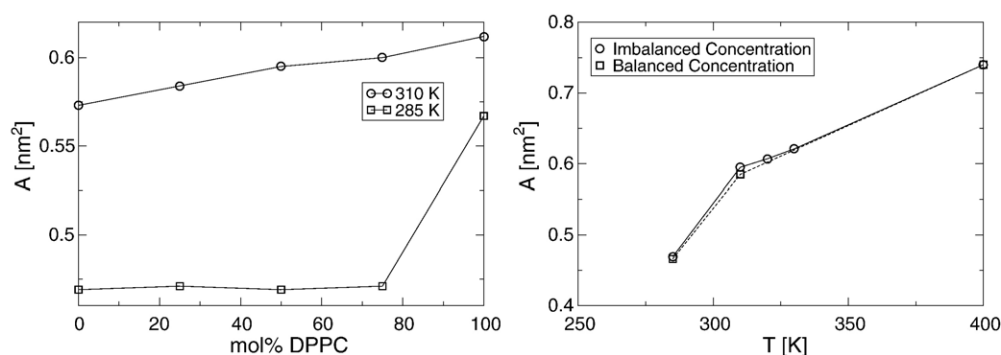


Fig. 1. Left: area per molecule versus concentration of DPPC for various temperatures. Right: area per molecule versus temperature for the equimolar mixture. Here we also compare the effects of different concentrations in the leaflets. Balanced means both leaflets have the same concentration. Imbalanced means a slight (<10%) difference in concentrations. Errors about 0.01 nm^2 . They have been determined by the standard block average technique [58].

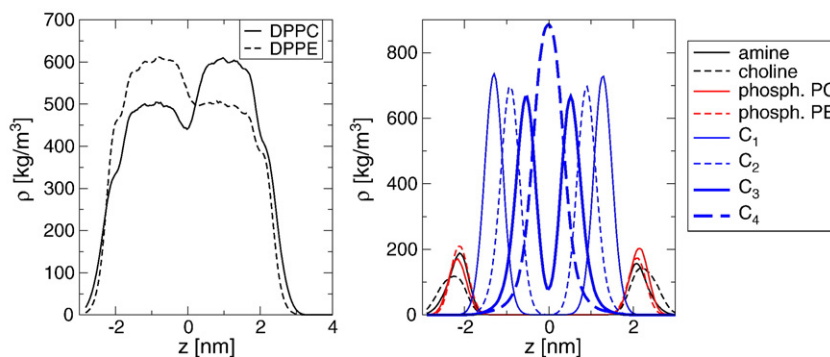


Fig. 2. Left: density profiles of the DPPC–DPPE bilayer at 310 K at equimolar concentration. $z=0$ is the center of the bilayer. Right: Density profile for 310 K at equimolar and balanced concentration resolved according to atomic groups.

temperatures (Fig. 1 Right) suggest that at 285 K the system is at least partially in the gel state. This is the first indication that the systems at the two main temperatures studied in this work are at qualitatively different points in the phase diagram. We see that the imbalance in lipid concentration has very little influence on the area per molecule. The only possible difference outside of the margin of error is right at the phase transition.

We show density profiles in Fig. 2. We find the well known shape of a density profile of a bilayer in water. The area of highest density is around the phosphate groups in the headgroup whereas the plane of smallest density is found in the middle of the bilayer where the tails from the opposing leaflets touch. This plane is also a symmetry plane of the system. The leaflets do not have necessarily equal concentrations as the distribution of DPPC and DPPE was set up randomly leading to asymmetric distributions if we study DPPC and DPPE density profiles separately.

Fig. 3 shows the density profiles of the hydrocarbon tails (C_1 – C_4) in the systems where we have equal concentration in the leaflets. It is interesting to note that the center of the bilayer has a higher density of DPPE than DPPC. Both lipids show a dip in the center, however, this is clearly more pronounced for DPPE. As DPPE can be expected to be more stretched out (below) it populates the center more strongly in order to avoid disrupting the headgroup layer to severely.

We see that there is some degree of interdigitation (Fig. 2 Right) between the leaflets as the C_4 atoms which are the ends of the tails in this representation generate a single central peak and even the C_3 atoms have a non-zero probability in the center of the bilayer. We can also identify that the headgroup conformation of PE and PC lipids is different from the average positions of the phosphate and amine or choline groups.

Fig. 4 shows the thickness of the bilayer derived from the density profiles. The thickness here is defined as the distance along the bilayer normal between the amine or choline peaks in the density profile. At 285 K sometimes we find a double peak structure in that cases the intermediate minimum is chosen for thickness calculations. We see in general that the thickness measured using the DPPC lipids is slightly larger than the one using the DPPE lipids. As both lipids are of the same length of the hydrophobic tails this may indicate a stronger stretching, i.e. higher ordering, of DPPC lipids (tails and/or headgroups), or weaker interdigitation. Again, here we

see a difference between temperatures. Comparing to Fig. 2 (right hand side) we conclude that the choline group is stronger delocalized and generally further sticking out into the water. At the higher temperature the bilayer is thinner. Generally we see a decrease of thickness with increasing PC concentration although this decrease is not completely monotonic. As was seen in Fig. 3 this thickness difference is dominated by the headgroups. The hydrocarbon thickness for DPPC and DPPE is the same within the error margins. Again we see a clear temperature influence.

As the thickness measure hints toward a conformational difference between the lipids we study the deuterium order parameters S_{CD} as measured by NMR in Fig. 5:

$$-S_{CD} = \frac{2}{3}S_{xx} + \frac{1}{3}S_{yy}, \quad (1)$$

$$S_{\alpha\beta} = \langle 3\cos\Theta_\alpha\cos\Theta_\beta - \delta_{\alpha\beta} \rangle, \quad \alpha, \beta = x, y, z \quad (2)$$

$$\cos\Theta_\alpha = \hat{e}_\alpha \hat{e}_z, \quad (3)$$

At the lower temperature the order is almost perfect, i.e. close to 0.5, whereas at 310 K the order is consistent with a liquid disordered state. On the other hand we do not see any indication of differences in order of the two lipids and only a slight difference between sn_1 and sn_2 chains. We have to keep in mind here that we can only expect semiquantitative or qualitative

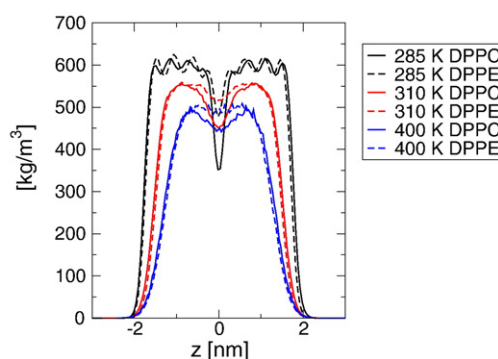


Fig. 3. Left: density profiles of the hydrocarbon tails of DPPC and DPPE at various temperatures at equimolar concentration with the same concentration in the leaflets. $z=0$ is the center of the bilayer.

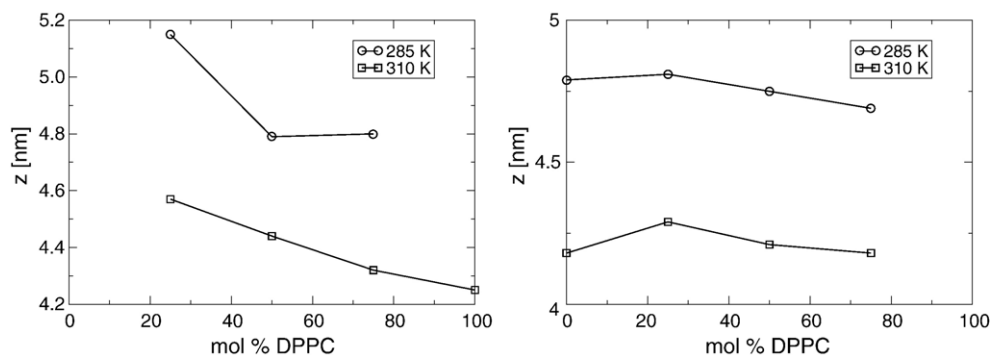


Fig. 4. Thickness of the bilayer measured between the maxima in the density profiles versus concentration of DPPC. Left: DPPC, Right: DPPE. Errors are about 0.05 nm as determined from the uncertainty in peak position in the density profile.

agreement between a coarse-grained model and experiments. The concentration dependence is a joint dependence that with increasing DPPE content the system altogether becomes more ordered affecting both lipids and both chains per lipid equally.

3.2. Dynamics

3.2.1. Global dynamics

We investigate two dynamical quantities in order to describe the overall dynamical behavior of the membranes. These are the mean-squared displacements (msds), leading to the diffusion behavior, and the reorientation dynamics. The lateral msds are shown in Fig. 6 leading to diffusion constants which are in the right order of magnitude for these systems (e.g. approx $1.5\text{--}2 \times 10^{-7} \text{ cm}^2/\text{s}$ for both DPPC and DPPE at 310 K in the equimolar mixture). We use the phosphate group to determine the msd. The temperature behavior is clearly visible. A concentration dependence or a different dynamics of the two constituents is at 310 K not discernible. The same is true at 285 K (not shown).

We now investigate the reorientation behavior. We use a vector connecting the two tails to each other measuring the in-plane rotation of the lipids. To this end we define a vector connecting the C_1 atoms of the two tails. This vector is almost perpendicular to the bilayer normal; it therefore decays to a value very close to zero. It cannot decorrelate completely as we

do not find trans-bilayer flip-flop on our timescales. We see that the concentration has only a weak influence on the reorientation in the fluid phase. Increasing DPPE concentration slightly slows down the reorientation of DPPE which can be explained by the decreasing area per molecule. This probably stems from the stronger interaction of DPPE headgroups which form a tighter and therefore more stable network [59]. The model does not include the hydrogen bonding capability in a local sense but it is designed to take this into account in an effective manner. We see that generally DPPE is slightly slower than DPPC under the same conditions consistent with the higher experimental higher phase transition and lower area. At 285 K the system is several orders of magnitude slower than at the higher temperature again consistent with expectations (Fig. 7).

We also study the reorientation of the headgroups (cf. Fig. 8), i.e. the vector connecting the phosphate to the amine or choline group. Again here we see that there is a clear temperature influence but weak influence of concentration. The reorientation is clearly faster than the lipid reorientation. All headgroups, including the ones belonging to the non-reorienting lipids (below), reorient on a few tens of ns. It is interesting to note that the reorientation process for the PC headgroups is faster but the residual order is higher. Due to the lack of flip-flops we again see a remaining memory of the initial orientation. This remaining orientation is in the PC case depending on temperature and concentration.

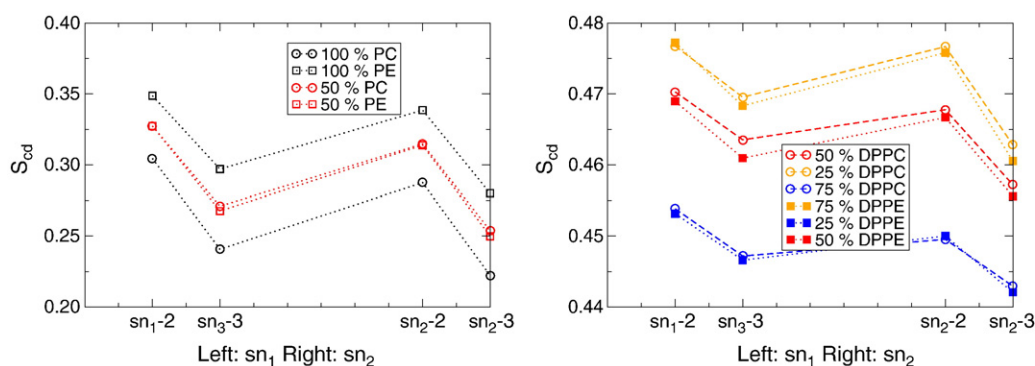


Fig. 5. Average order parameters in the bilayer: Left 310 K, Right: 285 K. In both figures the two left symbols correspond to the sn_1 chain and the right ones to the sn_2 chain. Order parameters are centered on C_2 , and C_3 as indicated. Error are about 0.001. We determined them by independently analyzing different parts of the trajectory.

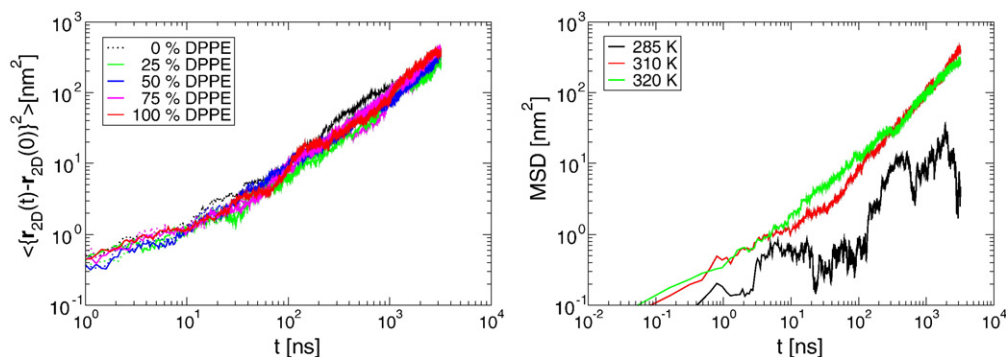


Fig. 6. Two-dimensional mean-squared displacements. Running time average has been applied. Left: depending on concentration at 310 K, full lines DPPC broken lines DPPE. Right DPPC at 25% DPPE and different temperatures.

3.2.2. Individual dynamics

Computer simulations have the advantage over experiments that they cannot only measure the average dynamics of the lipids but also the individual dynamical behaviors. The only compositions and temperature where we found a significant heterogeneity in the dynamics was the systems at 285 K with 75% DPPE or pure DPPE. The other concentrations at that temperature where pure gelphase and all the higher temperatures were clearly all liquid phase with homogeneous rapid reorientation.

The state points where we find heterogeneity are surprising as the experimental phase diagram shows that DPPE has a higher phase transition temperature [51] which would suggest if anything an increase in gel (or slow) population with PE concentration. But at 285 K we see the opposite. All other characteristics like the area per molecule and the order parameter indicate a highly ordered phase. It seems to be that this model yields a much more dynamically mobile ordered phase for PE than for PC. It should be noted that also the “fast” PE lipids at 285 K are orders of magnitude slower than PE lipids at 310 K. Fig. 9 shows all individual in plane reorientation correlation functions of all lipids at 75% PE and 285 K. We clearly see at least two distinct classes (marked in black and red), i.e. lipids which do not participate in the reorientation at all and lipids which reorient on the timescale of a few hundred nanoseconds. In order to exclude any problems with equilibra-

tion the system was equilibrated for 2 μ s before reorientation was analyzed.

3.3. Correlation between statics and dynamics

After we identified faster and smaller lipid populations it is of interest that we find a spatial (or other) relationship between dynamically like lipids. To this end we calculated radial distribution functions $g(r)$ between lipids of different dynamical identities. We do not consider lipids switching dynamic identities as clearly at least the slow lipids stay slow for the complete time. We focus on the dynamically separated system at 285 K and 75% DPPE where we already established the dynamic heterogeneity. We define now a lipid as “fast” if its reorientation correlation function has decayed to below 0.75 after 1 μ s and slow otherwise. This choice is somewhat arbitrary but motivated by the data as shown in Fig. 9. Similar to our recent analysis of a polymer system [60] we now correlate this dynamic heterogeneity with the static heterogeneity. We obtain that 24 out of 32 PC lipids are fast, i.e. 75%, and 78 out of 96 PE lipids are fast, i.e. 81%, indicating that there may be a weak tendency of the PE lipids to be on the fast side. In Fig. 10 we show radial distribution functions resolved according to fast and slow lipids where we clearly see that the fast and the slow lipids cluster. We use only the PO4 groups, i.e. the phosphates to calculate these rdfs. Also we see that generally there is only a

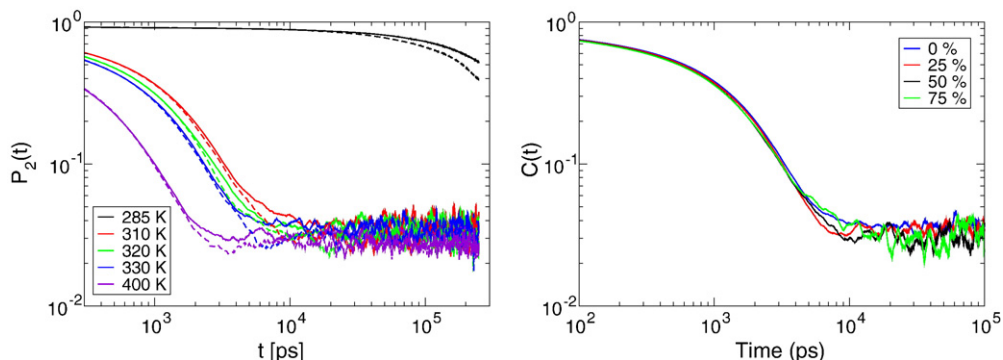


Fig. 7. Average reorientation of lipids at a 50:50 concentration. Left: in-plane reorientation. The DPPC lipids are solid lines and DPPE is denoted by dashed lines. Right: in-plane reorientation of DPPE lipids at 310 K depending on DPPC molar concentration. Note that these figures are on a double logarithmic scale in order to stress the small remaining order and long times involved.

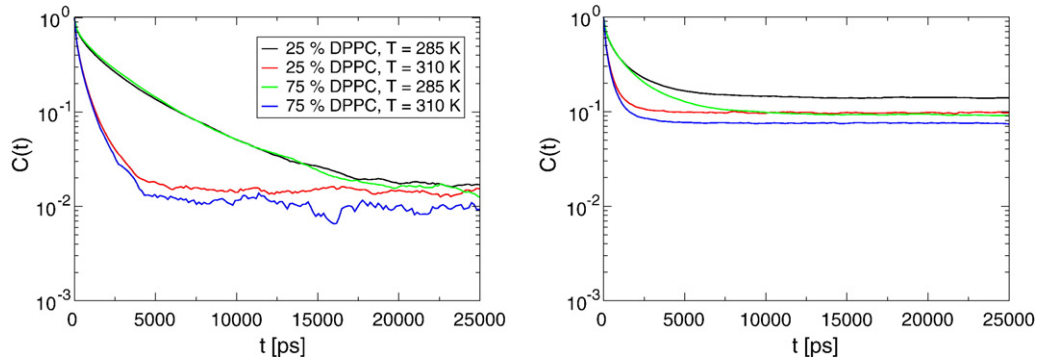


Fig. 8. Average reorientation of lipid headgroups. Left: DPPE, Right: DPPC. Legend applies to both sides.

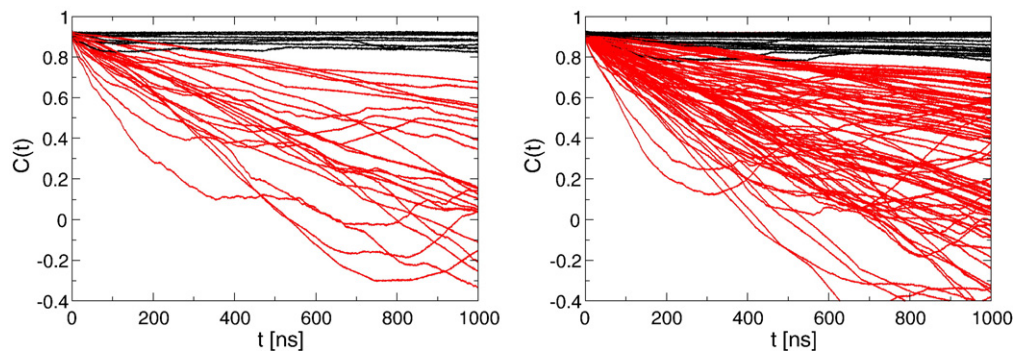


Fig. 9. Individual reorientation of lipids at 25:75 (PC:PE) concentration and 285 K. Left: DPPC, Right: DPPE.

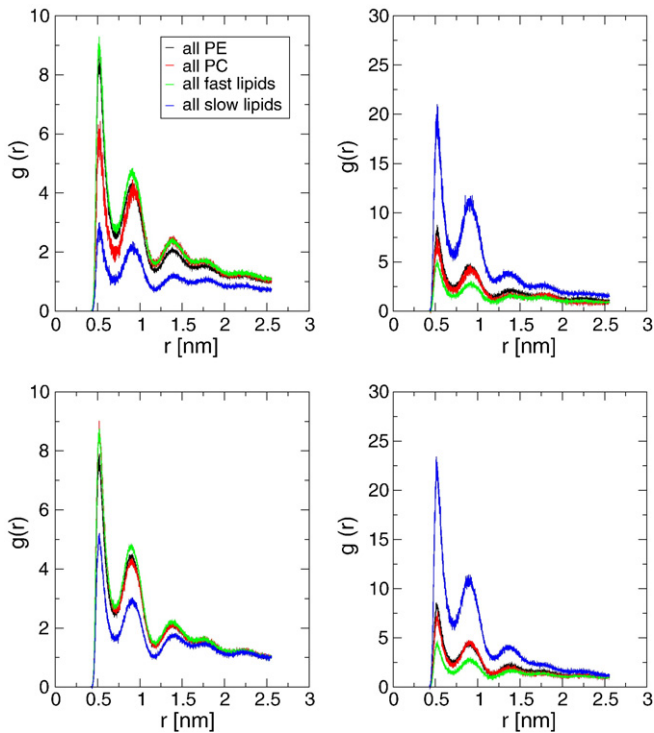


Fig. 10. Radial distribution functions $g(r)$ of dynamically defined classes in the system of 25% PC 75% PE at 285 K. Only the PO4 groups are considered. Top left: fast PC; top right: slow PC, bottom left: fast PE, bottom right: slow PE. The legend applies to all subfigures.

weak tendency of clustering of PE or PC lipids as the corresponding rdfs are similar indicating that there is strong mixing and that the separation is not in a way that all PE lipids are fast and all PC lipids slow.

We additionally calculate the order parameters of this system (cf. Fig. 11). The order of the PC lipids is for the middle of the chain, i.e. coarse grained atom 2–4, slightly larger than that of the PE lipids but more significantly we find that the slow lipids are more ordered than the fast lipids. Both are in the region of quite high order but there is a distinct difference.

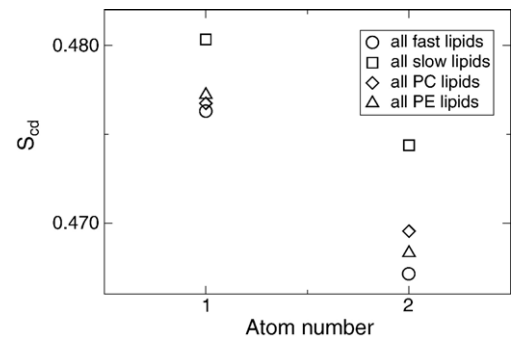


Fig. 11. Order parameters in the 25% DPPC 75% DPPE system at 285 K (sn_1 chains only). Fast and slow lipids are defined according to their reorientation dynamics, see text. Errors are about 0.001. We determined them by independently analyzing different parts of the trajectory.

4. Discussion

We studied the temperature and concentration effects in a DPPC/DPPE mixture using a well established coarse-grained lipid model. Overall we find the known behavior that this model semiquantitatively reproduces the phase behavior of lipid systems. The temperature differences to the experimental phase transition temperatures are about 20–30 K. We underestimate the phase transition temperatures. Increasing PE concentration leads generally to higher order and smaller area per molecule in agreement with atomistic simulations [53] and experiments [37,51,52]. This stems from the stronger interaction between the PE headgroups in contrast to PC headgroups. Especially the change in reorientation behavior with increasing PE shows this effect. Also the differences in thicknesses defined by headgroups and by tails shows that the headgroups are dominating the phase behavior in this case. The stronger interaction leads to a higher compression in the area and subsequently to increased order and a higher phase transition temperature.

At low temperatures we found a dynamically separated highly ordered phase. Although this may not be a 100% correct representation of a PC/PE lipid behavior the correlation between the static and dynamic heterogeneities are relevant for lipid mixtures. We can identify that the separation does not yield almost pure patches of the two lipids but only slight majority tendencies. This is in agreement with earlier findings using the same model for a mixture of PCs with different chain lengths [8]. We can clearly identify that in such a separated system there is a correlation between the order of a lipid and its dynamics, such that more highly ordered lipids are slower. Additionally we find a clear clustering of dynamic classes of lipids which is similar to the behavior in polymeric glass systems [60]. Such a dynamic clustering may be one of the underlying reasons for the formation of lipid rafts. Clearly for rafts more complex mixtures including also proteins are necessary but even in such a simple system we find a formation of very local dynamic clusters not leading to a perfect phase separation. It appears that at least in some cases the dynamics drives the separation rather than the thermodynamics. Our simulations are not yet long enough to characterize the lifetime of these structures but that is the next step necessary to gain a more complete understanding.

Acknowledgments

This work was partially supported by the National Science Foundation through NIRT grant BES 0506602.

References

- [1] L. Saiz, M.L. Klein, Computer simulation studies of model biological membranes, *Acc. Chem. Res.* 35 (6) (2002) 482–489.
- [2] H.L. Scott, Modeling the lipid component of membranes, *Curr. Opin. Struct. Biol.* 12 (4) (2002) 495–502.
- [3] M. Karplus, J.A. McCammon, Molecular dynamics simulations of biomolecules, *Nat. Struct. Biol.* 9 (9) (2002) 646–652.
- [4] R.W. Pastor, R.M. Venable, S.E. Feller, Lipid bilayers, NMR relaxation, and computer simulations, *Acc. Chem. Res.* 35 (6) (2002) 438–446.
- [5] S.O. Nielsen, C.F. Lopez, G. Srinivas, M.L. Klein, Coarse grain models and the computer simulation of soft materials, *J. Phys., Condens. Matter* 16 (15) (2004) R481–R512.
- [6] S. Izvekov, G.A. Voth, A multiscale coarse-graining method for biomolecular systems, *J. Phys. Chem., B* 109 (7) (2005) 2469–2473.
- [7] S.J. Marrink, A.H. de Vries, A. Mark, Coarse grained model for semi-quantitative lipid simulation, *J. Phys. Chem., B* 108 (2) (2004) 750–760.
- [8] R. Faller, S.-J. Marrink, Simulation of domain formation in mixed DLPC–DSPC lipid bilayers, *Langmuir* 20 (18) (2004) 7686–7693.
- [9] M. Edidin, Lipid microdomains in cell surface membranes, *Curr. Opin. Struct. Biol.* 7 (4) (1997) 528–532.
- [10] C. Dolainsky, P. Karakatsanis, T.M. Bayerl, Lipid domains as obstacles for lateral diffusion in supported bilayers probed at different time and length scales by two-dimensional exchange and field gradient solid state NMR, *Phys. Rev., E* 55 (4) (1997) 4512–4521.
- [11] M.C. Giocondi, V. Vie, E. Lesniewska, P.E. Milhiet, M. Zinke-Allmang, C. Le Grimmelc, Phase topology and growth of single domains in lipid bilayers, *Langmuir* 17 (5) (2001) 1653–1659.
- [12] T.V. Ratto, M.L. Longo, Obstructed diffusion in phase-separated supported lipid bilayers: a combined atomic force microscopy and fluorescence recovery after photobleaching approach, *Biophys. J.* 83 (6) (2002) 3380–3392.
- [13] Z. Feng, L. Chen, A. Chi-Keung, V. Chan, Effects of carbon chain difference and lipid composition on the contact mechanics of a two-component vesicle, *Colloids Surf., B Biointerfaces* 32 (1) (2003) 19–28.
- [14] J.V. Ricker, N.M. Tsvetkova, W.F. Wolkers, C. Leidy, F. Tablin, M. Longo, J.H. Crowe, Trehalose maintains phase separation in an airdried binary lipid mixture, *Biophys. J.* 84 (5) (2003) 3045–3051.
- [15] A. Arnold, M. Paris, M. Auger, Anomalous diffusion in a gel–fluid lipid environment: a combined solid-state NMR and obstructed random-walk perspective, *Biophys. J.* 87 (4) (2004) 2456–2469.
- [16] C. Gebhardt, H. Gruler, E. Sackmann, Domain-structure and local curvature in lipid bilayers and biological-membranes, *Z. Naturforsch., C* 32 (7–8) (1977) 581–596.
- [17] R. Krbecek, C. Gebhardt, H. Gruler, E. Sackmann, Three dimensional microscopic surface profiles of membranes reconstructed from freeze etching electron micrographs, *Biochim. Biophys. Acta, Biomembr.* 554 (1) (1979) 1–22.
- [18] S.L. Veatch, S.L. Keller, Separation of liquid phases in giant vesicles of ternary mixtures of phospholipids and cholesterol, *Biophys. J.* 85 (5) (2003) 3074–3083.
- [19] T. Baumgart, S.T. Hess, W.W. Webb, Imaging coexisting fluid domains in biomembrane models coupling curvature and line tension, *Nature* 425 (6960) (2003) 821–824.
- [20] S. Rozovsky, Y. Kaizuka, J.T. Groves, Formation and spatio-temporal evolution of periodic structures in lipid bilayers, *J. Am. Chem. Soc.* 127 (1) (2005) 36–37.
- [21] S.A. Pandit, D. Bostick, M.L. Berkowitz, Mixed bilayer containing dipalmitoylphosphatidylcholine and dipalmitoylphosphatidylserine: lipid complexation, ion binding, and electrostatics, *Biophys. J.* 85 (5) (2003) 3120–3131.
- [22] K. Balali-Mood, T.A. Harroun, J.P. Bradshaw, Molecular dynamics simulations of a mixed DOPC/DOPG bilayer, *Eur. Phys. J., E Soft Matter* 12 (S1) (2003) S135–S140.
- [23] A.H. de Vries, A.E. Mark, S.J. Marrink, The binary mixing behavior of phospholipids in a bilayer: a molecular dynamics study, *J. Phys. Chem., B* 108 (7) (2004) 2454–2463.
- [24] A. Gurtovenko, M. Patra, M. Karttunen, I. Vattulainen, Cationic DMPC/DMTAP lipid bilayers: molecular dynamics study, *Biophys. J.* 86 (6) (2004) 3461–3472.
- [25] K. Murzyn, T. Rog, M. Pasienkiewicz-Gierula, Phosphatidylethanolamine-phosphatidylglycerol bilayer as a model of the inner bacterial membrane, *Biophys. J.* 88 (2) (2005) 1091–1103.
- [26] B. Smit, P.A.J. Hilbers, K. Esselink, L.A.M. Rupert, N.M. van Os, A.G. Schlijper, Computer simulations of a water/oil interface in the presence of micelles, *Nature* 348 (6302) (1990) 624–625.
- [27] R. Goetz, G. Gompper, R. Lipowsky, Mobility and elasticity of selfassembled membranes, *Phys. Rev. Lett.* 81 (1) (1999) 221–224.

- [28] J.C. Shelley, M.Y. Shelley, R.C. Reeder, S. Bandyopadhyay, M.L. Klein, A coarse grain model for phospholipid simulations, *J. Phys. Chem., B* 105 (19) (2001) 4464–4470.
- [29] G. Ayton, G.A. Voth, Bridging microscopic and mesoscopic simulations of lipid bilayers, *Biophys. J.* 83 (6) (2002) 3357–3370.
- [30] M. Kranenburg, M. Venturoli, B. Smit, Phase behavior and induced interdigitation in bilayers studied with dissipative particle dynamics, *J. Phys. Chem., B* 107 (41) (2003) 11491–11501.
- [31] T. Murtola, E. Falck, M. Patra, M. Karttunen, I. Vattulainen, Coarse-grained model for phospholipid/cholesterol bilayer, *J. Chem. Phys.* 121 (18) (2004) 9156–9165.
- [32] M. Kranenburg, B. Smit, Phase behavior of model lipid bilayers, *J. Phys. Chem., B* 109 (14) (2005) 6553–6563.
- [33] K. Jorgensen, A. Klinger, R.L. Biltonen, Nonequilibrium lipid domain growth in the gel-fluid two-phase region of a DC₁₆PC–DC₂₂PC lipid mixture investigated by Monte Carlo computer simulation, FT-IR, and fluorescence spectroscopy, *J. Phys. Chem., B* 104 (4 9) (2000) 11763–11773.
- [34] E.I. Michonova-Alexova, I.P. Sugar, Size distribution of gel and fluid clusters in DMPC/DSPC lipid bilayers. A Monte Carlo simulation study, *J. Phys. Chem., B* 105 (41) (2001) 10076–10083.
- [35] E.I. Michonova-Alexova, I.P. Sugar, Component and state separation in DMPC/DSPC lipid bilayers: a Monte Carlo simulation study, *Biophys. J.* 83 (4) (2002) 1820–1833.
- [36] I.P. Sugar, R.L. Biltonen, Lateral diffusion of molecules in two-component lipid bilayer: a Monte-Carlo simulation study, *J. Phys. Chem., B* 109 (15) (2005) 7373–7386.
- [37] L.A. Bagatolli, E. Gratton, Two photon fluorescence microscopy of coexisting lipid domains in giant unilamellar vesicles of binary phospholipid mixtures, *Biophys. J.* 78 (1) (2000) 290–305.
- [38] C. Leidy, T. Kaasgaard, J.H. Crowe, O.G. Mouritsen, K. Jorgensen, Ripples and the formation of anisotropic lipid domains: Imaging two-component double bilayers by atomic force microscopy, *Biophys. J.* 83 (5) (2002) 2625–2633.
- [39] W. Lin, C. Blanchette, T.V. Ratto, M.L. Longo, Lipid asymmetry in dlpc/dspc supported lipid bilayers: a combined afm and fluorescence microscopy study, *Biophys. J.* 90 (1) (2006) 228–237.
- [40] D.A. Brown, E. London, Structure and origin of ordered lipid domains in biological membranes, *J. Membr. Biol.* 164 (2) (1998) 103–114.
- [41] K. Jacobson, C. Dietrich, Looking at lipid rafts? *Trends Cell Biol.* 9 (3) (1999) 87–91.
- [42] D.A. Brown, E. London, Structure and function of sphingolipid and cholesterol-rich membrane rafts, *J. Biol. Chem.* 275 (23) (2000) 17221–17224.
- [43] A. Pralle, P. Keller, E.L. Florin, K. Simons, J.K.H. Hörber, Sphingolipid-cholesterol rafts diffuse as small entities in the plasma membrane of mammalian cells, *J. Cell Biol.* 148 (5) (2000) 997–1007.
- [44] K. Simons, R. Ehehalt, Cholesterol, lipid rafts, and disease, *J. Clin. Invest.* 110 (5) (2002) 597–603.
- [45] L.J. Pike, Lipid rafts: heterogeneity on the high seas, *Biochem. J.* 378 (2) (2004) 281–292.
- [46] K. Simons, W.L. Vaz, Model systems, lipid rafts, and cell membranes, *Ann. Rev. Biophys. Biomol. Struct.* 33 (2004) 269–295.
- [47] K. Simons, E. Ikonen, Functional rafts in cell membranes, *Nature* 387 (6633) (1997) 569–572.
- [48] K. Simons, D. Tomre, Lipid rafts and signal transduction, *Nat. Rev., Mol. Cell. Biol.* 1 (1) (2000) 31–39.
- [49] J. Korlach, P. Schwille, W.W. Webb, G.W. Feigenson, Characterization of lipid bilayer phases by confocal microscopy and fluorescence correlation spectroscopy, *Proc. Natl. Acad. Sci. U. S. A.* 96 (15) (1999) 8461–8466.
- [50] C.A. Wolfe, P.S. James, A.R. Mackie, S. Ladha, R. Jones, Regionalized lipid diffusion in the plasma membrane of mammalian spermatozoa, *Biol. Reprod.* 59 (6) (1998) 1506–1514.
- [51] R. Mendelsohn, C.C. Koch, Deuterated phospholipids as raman spectroscopic probes of membrane structure. Phase diagrams for the dipalmitoyl phosphatidylcholine (and its d62 derivative)-dipalmitoyl phosphatidylethanolamine system, *Biochim. Biophys. Acta, Biomembr.* 598 (2) (1980) 260–271.
- [52] K. Arnold, A. L'osche, K. Gawrisch, ³¹P-NMR investigations of phase separation in phosphatidylcholine/phosphatidylethanolamine mixtures, *Biophys. Biochim. Acta, Biomembr.* 645 (1) (1982) 143–148.
- [53] S. Leekumjorn, A.K. Sum, Molecular simulation study of structural and dynamic properties of mixed DPPC/DPPE bilayers, *Biophys. J.* 90 (11) (2006) 3951–3965.
- [54] E. Lindahl, B. Hess, D. van der Spoel, GROMACS 3.0: a package for molecular simulation and trajectory analysis, *J. Mol. Model.* 7 (8) (2001) 306–317.
- [55] H.J.C. Berendsen, J.P.M. Postma, W.F. van Gunsteren, A. DiNola, J.R. Haak, Molecular dynamics with coupling to an external heat bath, *J. Chem. Phys.* 81 (8) (1984) 3684–3690.
- [56] A.N. Dickey, R. Faller, Investigating interactions of biomembranes and alcohols: a multiscale approach, *J. Polym. Sci., B* 43 (8) (2005) 1025–1032.
- [57] S.J. Marrink, J. Risselada, A.E. Mark, Simulation of gel phase formation and melting in lipid bilayers using a coarse grained model, *Chem. Phys. Lip.* 135 (2) (2005) 223–244.
- [58] M.P. Allen, D.J. Tildesley, *Computer Simulation of Liquids*, Clarendon Press, Oxford, 1987.
- [59] F. Suits, M.C. Pitman, S.E. Feller, Molecular dynamics investigation of the structural properties of phosphatidylethanolamine lipid bilayers, *J. Chem. Phys.* 122 (24) (2005) 244714.
- [60] R. Faller, Correlation of static and dynamic inhomogeneities in polymer mixtures: a computer simulation of polyisoprene and polystyrene, *Macromolecules* 37 (3) (2004) 1095–1101.